

# Prediction of wind load acting on telecommunication masts

## Márton BALCZÓ

Ph.D. Student  
Budapest University of  
Technology and  
Economics  
Budapest, Hungary  
[balczo@ara.bme.hu](mailto:balczo@ara.bme.hu)

## István GORICSÁN

Assistant Professor  
Budapest University of  
Technology and  
Economics  
Budapest, Hungary  
[goricsan@ara.bme.hu](mailto:goricsan@ara.bme.hu)

## Tamás KOVÁCS

Civil Engineer  
T-Mobile  
Budapest, Hungary  
[KOVACSTA@t-mobile.hu](mailto:KOVACSTA@t-mobile.hu)

## Tamás LAJOS

Professor  
Budapest University of  
Technology and  
Economics  
Budapest, Hungary  
[lajos@ara.bme.hu](mailto:lajos@ara.bme.hu)

## Tamás RÉGERT

Assistant Lecturer  
Budapest University of  
Technology and  
Economics  
Budapest, Hungary  
[regert@ara.bme.hu](mailto:regert@ara.bme.hu)

## Péter SEBESTYÉN

Civil Engineer  
Pannon-GSM  
Budapest, Hungary  
[PSebestyen@pgsm.hu](mailto:PSebestyen@pgsm.hu)

## Summary

Wind tunnel investigations on real structural components (legs, bracing members) and sections of telecommunication masts were carried out in order to provide reliable data for stress analysis necessary to design new masts or in case of an existing mast to define the useful load still available. The effect of wind turbulence and the roughness of the components on wind load was determined. The results show that in case of realistic atmospheric turbulence the drag coefficient of cylindrical components of regular surface treatment starts to decrease at  $Re = 4-6 \times 10^4$  (departure from sub-critical flow regime) and reaches its minimum (the supercritical flow regime) already at  $Re = 1-1.5 \times 10^5$ . In case of presence of atmospheric turbulence the increase of roughness of components by using various methods proved to be disadvantageous. Drag coefficients provided by numerical simulation of a mast section (FLUENT) agreed quite well with the measured ones.

**Keywords:** wind load, aerodynamic drag, telecommunication mast, turbulence intensity, super-critical flow, wind tunnel investigation, numerical simulation, CFD, laminar-turbulent transition

## 1. Introduction

Beside bridges the telecommunication masts have become the most frequently used and seen structures of civil engineering. Telecommunication service providers want to install more and more aeriels on their masts, so they are forced to share the infrastructure of their stations, so the payload of their masts with other companies. Installing new aeriels and cables is in most cases limited by the strength of the structures. To strengthen the weak points of the structures by using reasonable solutions is in most cases impossible (e.g. because of the hot dip galvanisation the components can not be welded). The replacement of the masts brings about considerable costs and disturbs the services.

In Hungary wind load constitutes the main load of light structures because the ice and rime load (and its simultaneity with high wind load) do not cause governing wind load combination. 50-70% of the wind load acts on the mast, the rest on the aeriels and cables. Significant economical and operational advantage would be realised if instead of strengthening or replacing existing mast a reserve in load capacity could be proved by calculating with realistic wind loads. Crash statistics show that the strength calculation of these structures is quite conservative. There are very few cases where masts collapsed, and the reasons for them are in most cases not the wind forces which were taken according to the standard into consideration at stress analyses, but coincidence of other fatal circumstances. According to an investigation [5] out of 225 mast failures in Europe only 7 were caused by wind overload. It is also thought-provoking that the wind-storm in 1999 in Denmark

caused no collapse of any masts although a number of masts should have been crashed according to the stress analyses carried out by using Eurocode.

While the stress analyses of masts relies on solid basis, the determination of loads, particularly the wind load depending on the effect of atmospheric turbulence, the surface roughness, the aerodynamic interaction of components, aeriels and cables is much less accurate and reliable. That is why telecommunication service provider Pannon GSM initiated in 2003 a wind tunnel investigation of aerodynamic load acting on real mast components (legs, bracing members, mast section) in order to explore the expected reserves in strength of masts. The results of the measurements were shared with two other service providers active in Hungary. As a consequence the third phase of the investigations was carried out together with T-Mobile in the Theodore von Kármán Wind Tunnel Laboratory of Department of Fluid Mechanics of Budapest University of Technology and Economics.

## 2. Flow past circular cylinders

The literature of flow past cylinders is very rich. There are publications which summarize the research results of a number of authors and define the state of the art in this field [1], [2], [3]. Two flow regimes past cylinders of size relevant to telecommunication mast structures ( $0,04 \leq D \text{ [m]} \leq 0,3$ ) can be differentiated: sub-critical and super-critical.

At sub-critical regime, for Reynolds number range  $Re < \sim 10^5$ , ( $Re = v_\infty D / \nu$  [-], where  $v_\infty$  [m/s] velocity of undisturbed flow (1),  $D$  [m] diameter,  $\nu$  [m<sup>2</sup>/s] kinematical viscosity) the boundary layer over the surface of the cylinder facing the wind is laminar so the ability of air to flow against adverse pressure gradient is very limited. Therefore the boundary layer separates relatively soon, at  $\varphi = 70 - 80^\circ$ , where  $\varphi$  [-] angle between the radii connecting the stagnation point over the front face of cylinder and the separation line with the axis of the cylinder. Consequently relatively large separation bubble develops behind the cylinder characterized by low pressure coefficient:  $c_p \cong -1$ , ( $c_p = 2(p - p_\infty) / \rho v_\infty^2$  [-], where  $(p - p_\infty)$  [Pa] the static pressure difference between the undisturbed flow and the local pressure,  $\rho$  [kg/m<sup>3</sup>] density) i.e. large depression, causing large drag  $c_D = 1.2$  (definition seen in (2)). Further characteristic of the wake is the periodic shedding of dynamic vortices (Karman vortex street) causing periodically fluctuating side force perpendicular to the undisturbed flow. The side force coefficient is large:  $c_s = 0.4 - 0.7$  ( $c_s = 2F_s / \rho v_\infty^2 DL$  [-] where  $F_s$  [N] side force,  $L$  [m] length), the Strouhal number characterizing the vortex shedding frequency  $St \cong 0.2$  ( $St = fD / v_\infty$  [-], where  $f$  [1/s] vortex shedding frequency). In range  $10^5 < Re < 3 \times 10^5$  transition of the flow field past cylinder occurs where the drag coefficient decreases continuously with increasing Reynolds number.

At supercritical regime ( $3 \times 10^5 < Re < 3 \times 10^6$ ) boundary layer over the front face of cylinder undergoes laminar – turbulent transition and because of enhanced momentum transfer in turbulent boundary layers the separation line shifts far downstream, to  $\varphi = 130 - 140^\circ$ . The size of the separation bubble and so the depression is much smaller than at sub-critical flow regime:  $c_p \cong -0.2$ . Consequently the drag coefficient is small:  $c_D = 0.3 - 0.4$ . No explicit vortex shedding can be observed and the side force coefficient is also small:  $c_s < 0.1$ .

Since the dramatic change of drag coefficient, i.e. the radical decrease of wind load is caused by flow phenomena in boundary layer that factors should be identified and influenced which control the flow in boundary layer. Besides the adverse pressure gradient the most decisive property of the boundary layer is the intensity of momentum transfer from the outside flow into the boundary layer that depends mostly on the laminar – turbulent character of the flow in boundary layer. The laminar-turbulent transition of boundary layers can be generated by increasing the Reynolds number, at given Reynolds number by increasing the turbulence of approaching flow and by increasing the relative roughness ( $k/D$ ) of the surface of the cylinder, where  $k$  [m] size of roughness of cylinder surface. The Reynolds number borders of sub- and supercritical flow regimes above belong to smooth cylinder surface and smooth (low turbulence) approaching flow. Extensive

investigations were carried out to determine the effect of these factors on the drag coefficient. It was found that the increase of both turbulence intensity and surface roughness decreases the upper border of sub-critical and lower border of supercritical flow regime, i.e. it shifts the transition from sub-critical to supercritical flow regime towards lower Reynolds number. At increased turbulence intensity and/or surface roughness when increasing Reynolds number the drag coefficient decreases and after reaching its minimum value (i.e. the supercritical regime at considerably smaller Reynolds number than in case of smooth flow and cylinder surface) the drag coefficient starts to increase. The higher is the turbulence intensity and surface roughness the higher is the value of drag in supercritical flow regime.

Although a number of publications addressing this subject are available, they give mainly qualitative information on flow processes and on relation between drag force and various factors. The incoherence of available data makes necessary to carry out experimental investigation on real components with usual surface treatment and roughness of the masts. The results of these measurements give solid basis for stress analyses.

### 3. Experimental setup

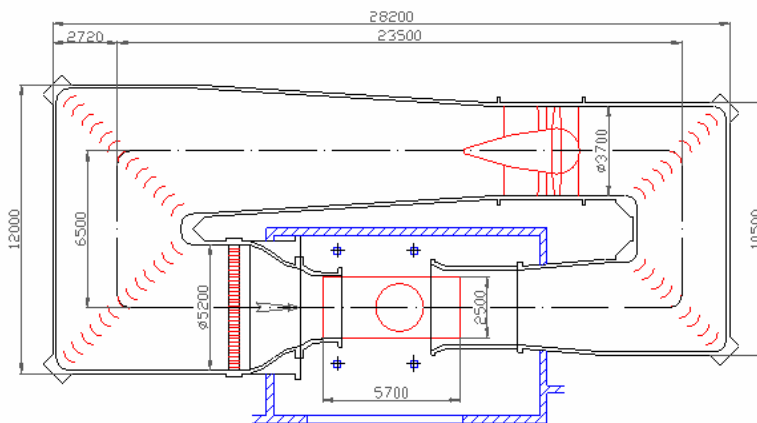


Fig. 1. The horizontal wind tunnel

Experimental investigations on the aerodynamic drag acting on components and sections of telecommunication masts were carried out in the test section of the horizontal recirculating wind tunnel with open test section of the Department of Fluid Mechanics of Budapest University of Technology and Economics (see Fig. 1.). Nozzle diameter and length of test section is 2.6 m and 5.7 m, respectively, the maximum wind velocity is 60 m/s, turbulence intensity in the empty test section is  $Tu = 0.45\%$ .

The model was put in a uniform flow of three different turbulence levels: smooth, low turbulence ( $Tu = 0.45\%$ ) flow, and turbulent flows of 5% and 7.5% turbulence intensity. This turbulence intensity corresponds to the turbulence of atmospheric boundary layer corresponding to undisturbed open-country environment (smooth terrain) at about 50 m height. (At smaller height and rougher terrain the turbulence intensity is bigger.) The turbulence intensity was enhanced by a grid fixed in the outlet cross section of the nozzle (see Fig. 2.)

Fig. 2. shows also a cylindrical mast component in the test section of wind tunnel. In order to ensure a 2D (two-dimensional) flow, the model was fixed between two end-plates (see Fig. 2.) fixed to a frame. The component was suspended on the frame on both ends via its shafts and two vertical rods having 2-2 spherical joints.

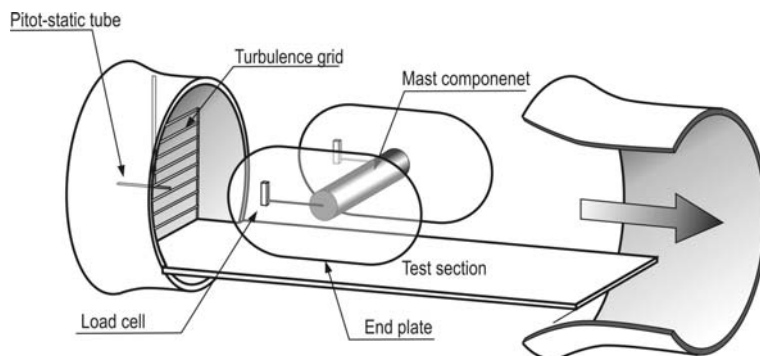


Fig. 2. Drag measurement setup

These shafts were connected also by two horizontal rods provided with 2-2 spherical joints at their ends to two load cells measuring the drag forces. The measuring system was calibrated before and after each measurement. In order to fix the model against rotation around its axis in case of non-cylindrical components or mast sections, the shaft of the model was fixed by a special grasping part fixed to the horizontal bar.

So the moment of air forces did not generate horizontal force component, influencing the drag measurement. The shafts and rods were sheltered against wind forces.

The measurement of drag force ( $F_D$ ) was carried out by two calibrated load cells connected to the ends of the cylinders. The force data were captured for 20 s with 500 Hz frequency and processed by a PC. The wind velocity in the test section ( $v_{ref}$  [m/s]) was determined by measuring the difference of the total pressure (head,  $p_t$  [Pa]) in the inlet of wind tunnel nozzle by a row of Pitot tubes and the static pressure in the test section ( $p_0$  [Pa]), i.e. the dynamic pressure  $p_{dyn} = (p_t - p_0)$  [Pa]. The pressure difference was measured with pressure transducers (20 s, 500 Hz).

The undisturbed (approaching) wind velocity was calculated from the measured dynamic pressure:

$$v_{\infty} = \sqrt{\frac{2}{\rho} p_{dyn}} \quad (1)$$

The drag coefficient  $c_D$  was determined from

$$c_D = \frac{F_D}{p_{dyn} D L} \quad (2)$$

where  $F_D$  [N] is the drag force,  $D$  [m] and is the diameter (or characteristic size) of the component and  $L$  [m] is its length perpendicular to the wind direction. For each component and Reynolds number the mean of 10000 drag coefficients was determined. The turbulence intensity was measured by constant temperature hot wire anemometer.

## 4. Results

Cylindrical components of diameter  $D$ [mm] = 48 (H), 89 (H), 114 (HP), 168 (H), 245 (HP) were measured, where H and P letters relate to hot dip galvanized and painted surfaces, respectively. The turbulence intensity was varied: 0.45 % (without turbulence generators), 5% and 7.5% (with two different turbulence generators).

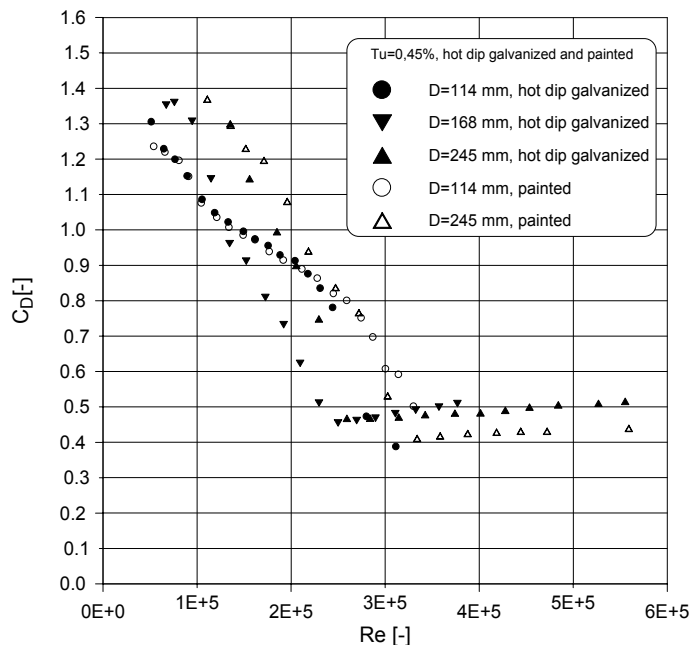


Fig. 3. Drag coefficient versus Reynolds number at low turbulence intensity at different relative roughness of the components

Fig. 3. shows the change of the drag of components (circular cylinders) of different diameters versus Reynolds number. The surface of the components was prepared by using two different surface treatments: hot dip galvanization and painting. In contrast to painting the former treatment causes larger and significantly variable roughness. The measurement was carried out at low 0.45 % turbulence intensity. The departure from sub-critical flow regime, i.e. the decrease of  $c_D$  with increasing  $Re$  starts at  $Re = 0.5 - 0.8 \times 10^5$ . According the expectations the supercritical regime characterized by the lowest drag coefficient ( $c_D=0.46$ ) is reached at lowest  $Re$  ( $2.6 - 2.8 \times 10^5$ ) by components of larger relative surface roughness  $k/D$  (with hot dip galvanisation, filled symbols). The painted components of smooth surface reaches the supercritical flow regime the lowest  $c_D$  (0.4) at higher Reynolds number ( $Re = 3.3 \times 10^5$ ). When increasing further the Reynolds

number drag coefficient increases at all components slightly: in the investigated  $Re$  range  $\Delta c_D = 0.03 - 0.04$ .

Fig.4. is similar to Fig.3. more components of different diameters with painted (open symbols) and hot dip galvanised (filled symbols) surfaces were investigated but the turbulence intensity was much higher:  $Tu = 5\%$ . The increase of turbulence caused a significant change: the departure from sub-critical flow regime occurs already at  $Re = 0.3 - 0.5 \times 10^5$  both at components of smooth and rougher surface. With increasing Reynolds number the drag coefficient decreases much steeper than at small turbulence intensity and reaches the minimum value ( $C_{Dmin} = 0.37 - 0.48$ , depending on the relative roughness), i.e. the supercritical flow regime at  $Re = 1-1.5 \times 10^5$ . At higher turbulence intensity the surface roughness does not have significant impact on the sub-supercritical transient regime. In contrast to this observation in supercritical regime the increase of  $c_D$  with increasing Reynolds number is much steeper at bigger relative roughness than at smooth (painted) surface. So at larger Reynolds numbers considerably higher drag coefficient ( $\Delta c_D = 0.08 - 0.1$ ) can be observed at hot

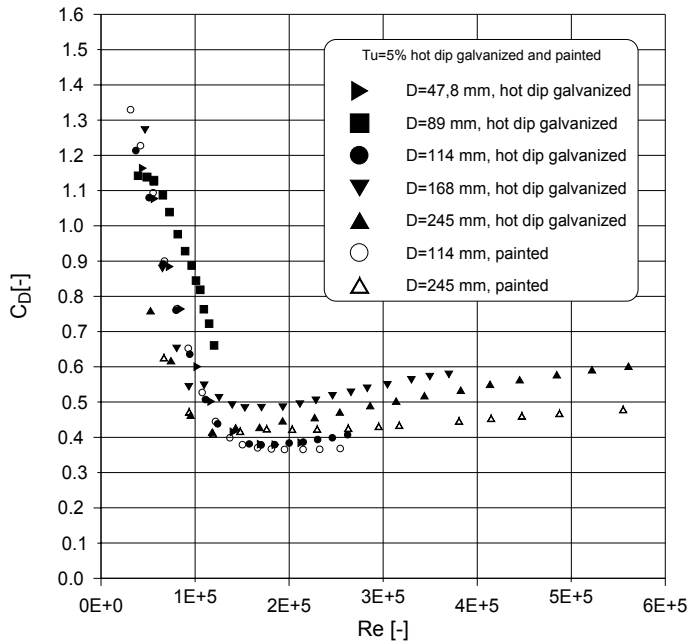


Fig. 4. Drag coefficient of components at higher (5%) turbulence intensity

dip galvanised than at painted surface of components of the same diameter.

In Fig.5. the drag - Reynolds number relation can be seen at mast component of  $D = 245$  mm diameter at three different turbulence intensities ( $Tu = 0,45\%$ ,  $5\%$  and  $7.5\%$ ) and two surface roughness. A very significant influence of turbulence intensity can be observed. In case of low turbulence flow ( $Tu = 0,45\%$ ) the supercritical flow regime occurs at  $Re 3.3 \times 10^5$  and  $2.6 \times 10^5$  in case of painted and hot dip galvanized surface, respectively. At smooth (painted) surface and  $Tu = 5\%$  and  $7.5\%$  turbulence intensity the supercritical flow regime ( $C_{Dmin} = 0.41$  and  $0.34$ ) is reached at  $Re = 1.2 \times 10^5$  and  $0.9 \times 10^5$ , respectively. At higher turbulence intensity the roughness of surface influences the drag: at  $Tu = 7.5\%$  the difference between the drag for hot dip galvanised and painted surface was  $\Delta c_D = 0.05-0.1$ . In supercritical flow regime the drag increases with increasing Reynolds number. The higher is the turbulence intensity and the surface roughness the steeper is the change.

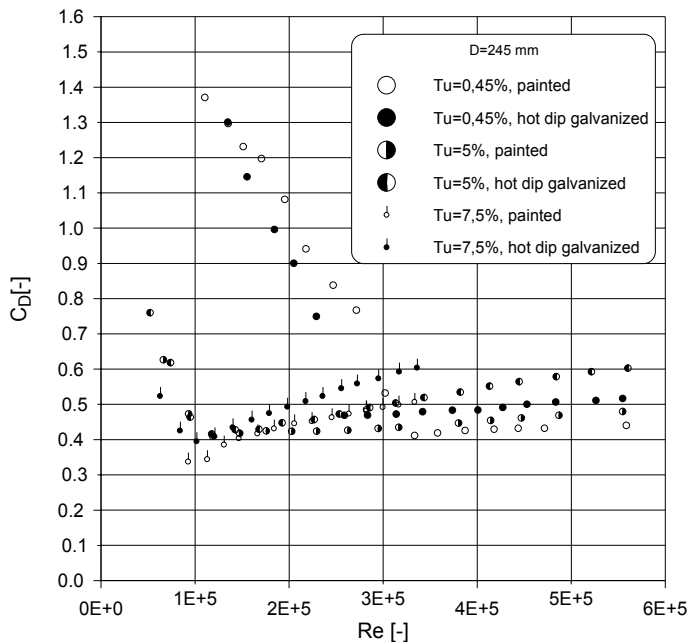


Fig. 5. Effect of turbulence intensity and surface roughness on the drag of a mast component

Wind tunnel measurements were carried out to investigate the effect of surface roughness on the drag. A cylindrical component of  $D = 114$  mm diameter was measured. At smooth (painted) surface the measurement was carried out at three different turbulence intensities. Similar experiences were collected as at measurement with component of diameter  $D = 245$  mm (see Fig. 5.). Various roughness elements (meshes, spiral wire and sandpaper) were fixed to the surface of the component and the drag was measured at low ( $0.45\%$ ) turbulence intensity of the flow. The result shows

at  $Tu = 7.5\%$  the difference between the drag for hot dip galvanised and painted surface was  $\Delta c_D = 0.05-0.1$ . In supercritical flow regime the drag increases with increasing Reynolds number. The higher is the turbulence intensity and the surface roughness the steeper is the change.

that as effect of roughness elements the sub – supercritical transition starts at relatively small Reynolds number but the drag belonging to supercritical flow regime is much higher than at of painted or hot dip galvanized surfaces ( $c_D= 0.9$  instead of 0.37-0.45, see Fig. 4.). Both wind tunnel measurements and numerical simulations were carried out also on a mast section shown in Fig.6.

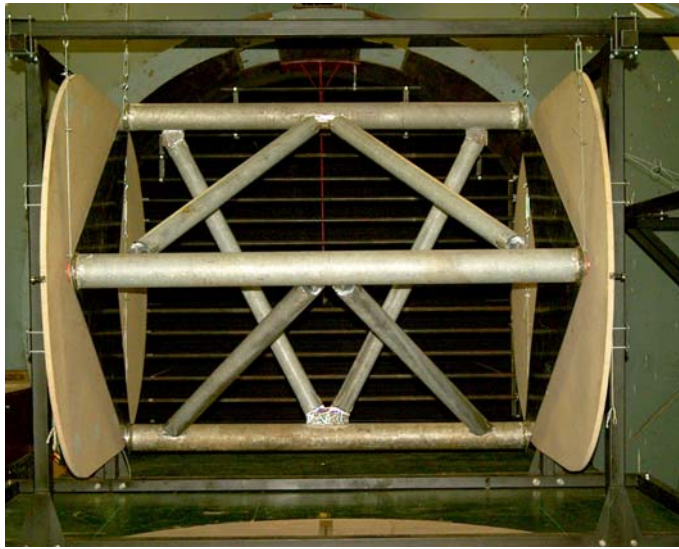


Fig. 6. Mast section in the wind tunnel

The results shown by the diagram is in harmony with the results of measurements of isolated mast components. The average drag coefficient related to legs and bracing members can be estimated by dividing the  $c_D$  related to the mast section (Fig.7.) by 1.5: at  $Re_{legs} = 10^5$  and  $2 \times 10^5$  ( $Re_{bracing\ members} = 0.7$  and  $1.4 \times 10^5$ )  $c_{D\ mean} = 0.7$  and 0.53, respectively. Good agreement can be found when comparing these estimated drag coefficient to that plotted in Fig.4. for hot dip galvanized cylinders. This experiment seems to verify the adaptability of results of measurements of components for calculating the drag acting on the mast.

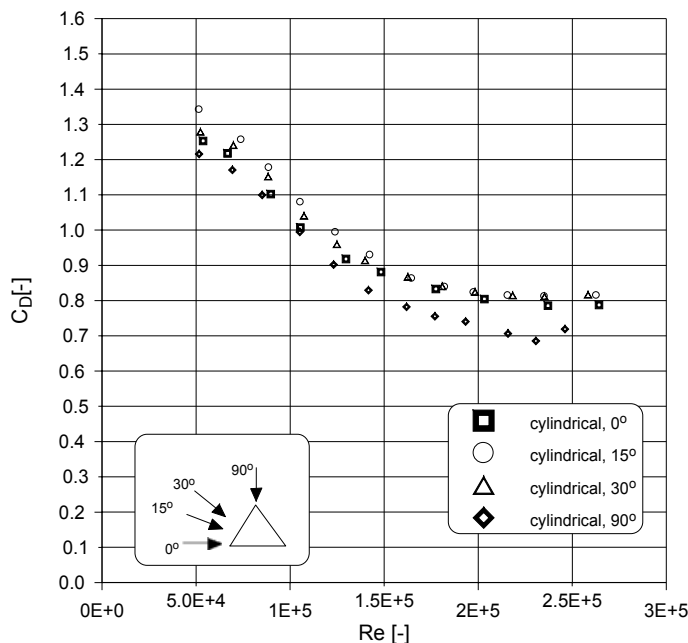


Fig.7. Drag coefficient of mast section

Both wind tunnel measurements and numerical simulations were carried out also on a mast section shown in Fig.6. The diameter of the hot dip galvanized legs and bracing members of was  $D = 108$  and 75 mm, respectively. The results of the measurements at  $Tu = 5\%$  turbulence intensity are shown on Fig. 7., where the Reynolds number and the drag coefficient were calculated with the diameter of the leg and with the projected area of two legs and two bracing members constituting one side of the mast of triangular cross section, respectively.

The results shown by the diagram is in harmony with the results of measurements of isolated mast components. The average drag coefficient related to legs and bracing members can be estimated by dividing the  $c_D$  related to the mast section (Fig.7.) by 1.5: at  $Re_{legs} = 10^5$  and  $2 \times 10^5$  ( $Re_{bracing\ members} = 0.7$  and  $1.4 \times 10^5$ )  $c_{D\ mean} = 0.7$  and 0.53, respectively. Good agreement can be found when comparing these estimated drag coefficient to that plotted in Fig.4. for hot dip galvanized cylinders. This experiment seems to verify the adaptability of results of measurements of components for calculating the drag acting on the mast.

Numerical simulation of the flow past mast section shown in Fig.6. was carried out with FLUENT 6.2 code at two wind directions ( $0^\circ$  and  $90^\circ$ , see Fig.7.). Because of the symmetry only half of the section was considered. Fig.8. shows the flow domain and the mesh. The flow domain contained also the fixed plate at the lower portion of the wind tunnel test section. The end plates were taken into account as slip wall boundary conditions. At the surface of the cylindrical legs the boundary layer was treated carefully by using prismatic numerical cell layers. The grid consisted of 760000 tetrahedral cells and computations were made on two parallel computational processors. The computations were carried out in 3-dimensional space and the Reynolds Averaged Navier Stokes (RANS) equations were solved simultaneously with the continuity equation. The

appearing turbulent Reynolds stresses were modelled via the isotropic, eddy viscosity concept, using the 'realizable'  $k-\epsilon$  turbulence model. At the near wall region this turbulence model is not valid, thus logarithmic wall functions were applied there which were corrected by the pressure gradient effects. For that reason, the grid was created to achieve  $y^+ \approx 30-50$  non-dimensional wall distance ( $y^+ = y \cdot u_\tau / \nu$  where  $u_\tau$  is the friction velocity,  $\nu$  is the kinematical viscosity of the air) at the first layer of cells neighbouring the wall surface.

The inlet boundary condition was a prescribed uniform averaged velocity profile that provided  $Re_D = 2.2 \times 10^5$  Reynolds number based on the diameter of the leg. The outlet part of the computational domain was  $50 D$  far downstream from the mast section where constant static pressure was prescribed. The flow-parallel sides of the computational domain were slip walls.

The turbulence models caused a restriction in the simulated cases to be placed only in the supercritical domain, where the boundary layer on the surfaces of the legs and bracing members are fully turbulent.

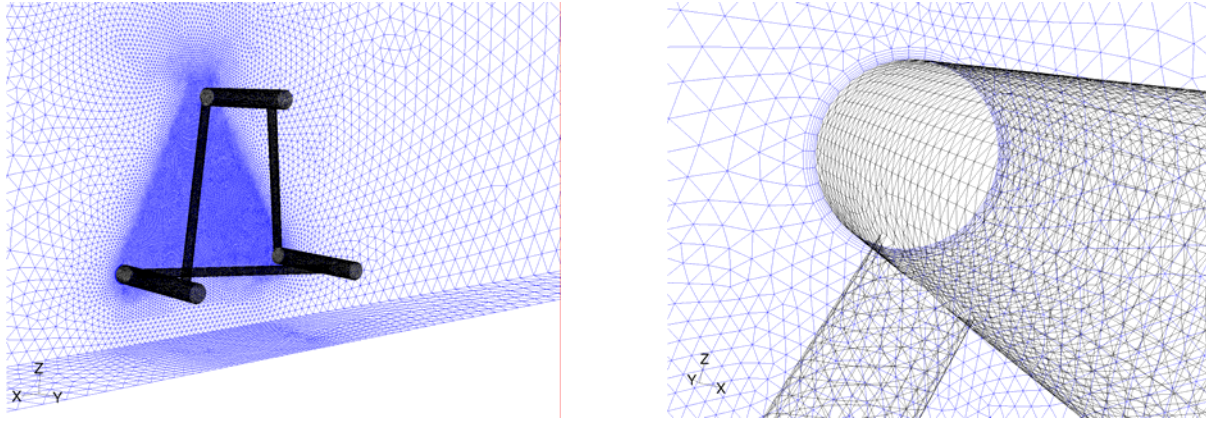


Fig. 8. Flow domain and the mesh around the mast section

The mast segment was rotated similarly to the experiments to obtain an angle of attack of  $90^\circ$ , thus other parts of the computational domain were unaffected by changes. The force acting on the mast segment was computed by integration of the pressure and shear stress distributions on its surfaces. The static pressure distribution on the mast surfaces for both angles of attack can be seen in Fig. 9.

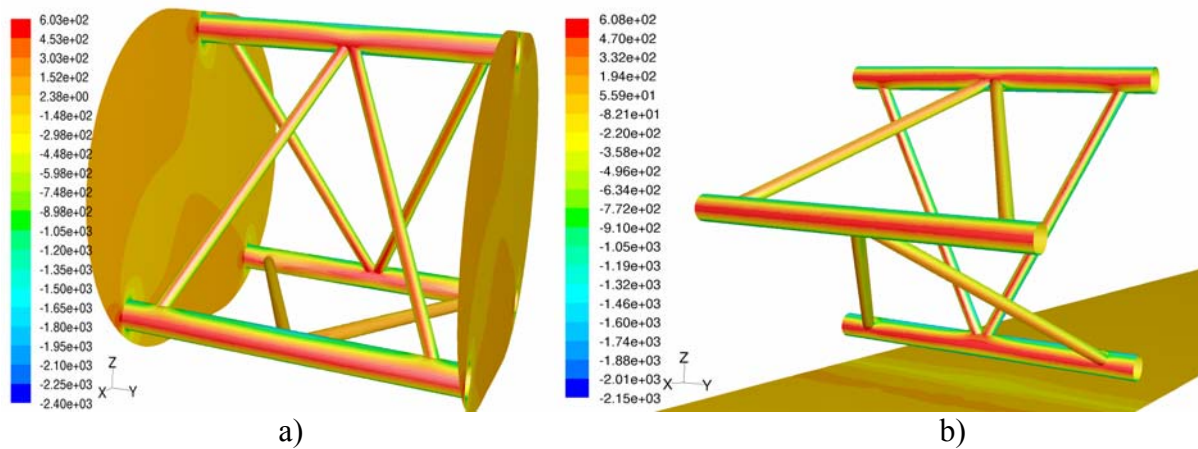


Fig. 9. Static pressure distribution on the surface of the mast segment. The upstream sides are shown, flow from lower left to upper right. a)  $0^\circ$ , b)  $90^\circ$  angle of attack

For the computation of the drag coefficients the reference value of the velocity was  $30 \text{ m/s}$ , reference area  $A_{ref} = 0.651 \text{ m}^2$ . The drag coefficient for  $0^\circ$  and for  $90^\circ$  angle of attack was computed to be  $c_D = 0.71$  and  $0.69$ , respectively. The measured values at  $0^\circ$  and  $90^\circ$  angle of attack were  $c_D = 0.79$  and  $0.71$ , respectively. While at angle of attack  $0^\circ$  the simulation overestimate the drag by 10% at  $90^\circ$  the agreement is very good ( $\Delta c_D = 0.02$ ). The numerical simulation of the flow past the whole mast could take the environment (vegetation, features of terrain, buildings) as well as the forces acting on and the sheltering effect of aeriels, cables into account giving most reliable and realistic load data for stress analyses.

## 5. Conclusions

Based on investigation the following conclusions can be formulated: the departure from the sub-critical flow regime characterised by high drag ( $c_D = 1.2$ ) occurs at  $Re = 0.5-1 \times 10^5$  independent from turbulence intensity of the approaching flow and surface roughness of the components. In case of low turbulence flow and smooth surface the sub - supercritical transition takes place in a quite large ( $\geq 2 \times 10^5$ ) Reynolds number range: the aerodynamic drag acting on circular cylinders reaches its minimum value (the supercritical flow regime) at relatively high Reynolds number  $Re \geq 3 \times 10^5$ .

Besides increasing the Reynolds number there are two means with which the Reynolds number range of this transition can be considerably shortened, i.e. the supercritical flow regime with low drag coefficient can be reached: increase of surface roughness and increase of turbulence intensity of the approaching flow. Significant reduction of this Reynolds number range can be achieved with large relative roughness, but the drag belonging to supercritical domain is relatively high:  $c_D = 0.8-0.9$ , due to the effect of roughness on the flow.

The increased turbulence intensity of approaching flow shortens the Reynolds number range of transition without significant increase of the drag forces in supercritical domain in contrast to low turbulence intensity (see Figs. 4. and 5.). According to the investigations reported here the supercritical flow regime with low ( $c_D = 0.4-0.5$ ) drag can be achieved at  $Tu = 5\%$  turbulence intensity already at  $Re = 1 - 1.5 \times 10^5$ . This turbulence intensity is present at all ground roughness in the lower part (height over the ground  $\leq 80$  m) of atmospheric boundary layer [4]. In addition, in case of downstream component of the masts the atmospheric turbulence is enhanced by the turbulence caused by upstream components. So the stress analyses of masts can be based on a supercritical Reynolds number range starting at  $Re = 1 - 1.5 \times 10^5$ . These conclusions are in harmony with the statement of relevant literature [1], [2], [3]. Comparative analysis proved that calculations carried out on the basis of Eurocode, using the findings of our wind tunnel tests result 5-20% savings in the different structural elements of a mast compared to the calculations based on Hungarian Standards. As an immediate gain Pannon did not have to change a heavily loaded tower and avoided serious costs and disturbance of its services.

The experiment on mast section seems to verify the adaptability of results of measurements of components for calculating the drag acting on the whole mast. Numerical simulation of the flow past mast section provided encouraging results. Further studies are needed to developing a reliable CFD model with which the wind force acting on mast and aerials and cables can be predicted with necessary accuracy.

## 6. References

- [1] RUSCHEWEYH, H. *Dynamische Windwirkung an Bauwerken*, Band 1. Bauverlag GmbH, Wiesbaden, Berlin
- [2] ZDRAVKOVICH, M. M. *Flow around circular cylinders, Vol. 2. Applications*
- [3] SUMER, M. B., FREDSOE, J. *Hydrodynamics around cylindrical surfaces*, World Scientific Publishing Company, Singapore, 1999
- [4] Umweltmeteorologie, *Physikalische Modellierung von Strömungs- und Ausbreitungsvorgängen in der atmosphärischen Grenzschicht VDI 3783 Blatt 12*. Entwurf, 1999.
- [5] LAIHOT, J. *IASS Working Group IV Masts and Towers 19th Meeting in Cracow, Poland, Materials and proceedings*, Cracow University of Technology, 2000